

1 **1. Title page**2 **Sequestering carbon in the subsoil benefits crop transpiration at the**  
3 **onset of drought**4  
5 Maria Eliza Turek<sup>1,2,\*</sup>, Attila Nemes<sup>3,4</sup>, Annelie Holzkämper<sup>1,2</sup>6  
7 <sup>1</sup> Agroscope, Division of Agroecology and Environment, Zürich, Switzerland8 <sup>2</sup> University of Bern, Oeschger Centre for Climate Change Research, Bern, Switzerland9 <sup>3</sup> Norwegian University of Life Sciences, Faculty of Environment and Natural Resource  
10 Management, Ås, Norway11 <sup>4</sup> Norwegian Institute of Bioeconomy Research (NIBIO), Division of Environment and Natural  
12 Resources, Ås, Norway

13 \*Corresponding author

14 E-mail: [mariaeliza.turek@agroscope.admin.ch](mailto:mariaeliza.turek@agroscope.admin.ch)15 [Attila.Nemes@nibio.no](mailto:Attila.Nemes@nibio.no)

16 annelie.holzkaemper@agroscope.admin.ch

17

18

19

20      **2. Abstract**

21      Increasing soil organic carbon is promoted as a negative emission technology for the  
22      agricultural sector with a potential co-benefit for climate adaptation due to increased soil  
23      water retention. Field-scale hydrological models are powerful tools to evaluate how the  
24      agricultural systems would respond to the changing climate in upcoming years and  
25      decades, to predict impacts, and look for measures that help decrease drought-driven crop  
26      stress under current and future climatic conditions. We quantified how different levels of  
27      soil organic carbon (SOC) additions at varied soil depths are expected to influence  
28      drought-induced transpiration reduction ( $T_{redry}$ ) in maize cultivated in Switzerland.  
29      Parameterization of the model based on a pedotransfer function (PTF) was validated  
30      against soil moisture data from a long-term lysimeter experiment with a typical Swiss soil  
31      and the model was subsequently applied under climate forcing between 1981 until 2099  
32      representative of three distinct climatic sites of Switzerland. We used the same PTF to  
33      indirectly assess the effects of SOC additions in different depths on soil hydraulic  
34      properties. We found a threshold in both added amount of SOC (2% added) and in the  
35      depth of sequestering that SOC (top 65cm) beyond which any additional benefit appears  
36      to be substantially reduced. However, adding at least 2% SOC down to at least 65 cm  
37      depth can reduce  $T_{redry}$  in maize, i.e. increase transpiration annually, but mostly at the  
38      onset of summer drought by almost 40 mm. We argue that SOC increases in subsoils can  
39      play a supporting role in mitigating drought impacts in rain-fed cropping in Switzerland.  
40

41      Keywords: climate change adaptation; water use efficiency; soil management;  
42      pedotransfer functions, simulation modeling; SWAP

43 

### 3. Introduction

44 Over the last few decades, scientific studies have increasingly emphasized the  
45 need and explored potentials for soil carbon sequestration in agricultural soils to mitigate  
46 climate change (e.g. Lal (2001, 2004); Minasny et al. (2017); Smith et al. (2008)). In this  
47 context, other possible impacts of increasing soil organic carbon (SOC) on important soil  
48 functions and services have also been highlighted (e.g. on soil biodiversity, soil structure,  
49 soil water retention and infiltration capacity; see Lal (2004); Murphy (2015)).  
50 Management practices such as application of organic amendments (i.e. compost, manure,  
51 biochar), cover cropping, crop diversification and the adoption of conservation tillage  
52 systems are commonly considered beneficial for increasing SOC (Crystal-Ornelas et al.,  
53 2021). With an increase in soil organic carbon in quantity, quality and chemical diversity,  
54 soil communities are promoted and biotic-abiotic interactions are enhanced, with positive  
55 impacts on the formation and storage of soil organic matter (Zhang et al., 2021). Physical  
56 properties of the soil are altered directly by soil organic carbon increase and indirectly  
57 through the activity of soil fauna (e.g. Arthur et al. (2015); Rivier et al. (2022); Nemes et  
58 al. (2005); Rawls et al. (2004)). Soil structure has major influence on the natural soil water  
59 retention capacity, an essential regulating ecosystem service provided by soils that may  
60 play an increasingly crucial role in mitigating drought-induced limitations as climate  
61 change progresses (Liu et al., 2021). Soil texture also strongly affects how soil hydraulic  
62 properties respond to organic amendments, as shown by a meta-analysis from Edeh et al.  
63 (2020), who reported decreased hydraulic conductivity of sandy soils and increased the  
64 hydraulic conductivity of clayey soils after biochar additions. A recent meta-analysis  
65 performed for Europe has also shown that the adoption of organic amendments and  
66 “continuous living cover” benefit the soil water regulation functions (Blanchy et al.,  
67 2023).

68 With that in mind, the potential for achieving synergies between climate  
69 mitigation and adaptation seem promising. However, empirical evidence on benefits from  
70 increasing soil organic carbon for reducing drought limitations in crops is inconclusive.  
71 For example, Minasny and Mcbratney (2017) performed a meta-analysis with globally  
72 distributed soil data combined with the development of pedotransfer functions (PTFs) and  
73 found that 1% increase in SOC has a minor effect on available water capacity (AWC),  
74 with more pronounced differences in sandy soils than fine textured soils. Libohova et al.  
75 (2018), however, evaluated the effect of SOC on AWC using the National Cooperative  
76 Soil Survey (NCSS) Soil Characterization Database and found that a 1% increase in soil  
77 organic matter content increased AWC up to 1.5% times its weight, depending on soil  
78 texture and clay mineralogy. Also, a global metanalysis of 17 long-term field experiments  
79 conducted by Eden et al. (2017) found that plant available water increased significantly  
80 with the addition of organic material to the topsoil.

81 So far, only few model-based analyses have explored benefits of SOC increases  
82 on soil water availability systematically. Thereby, assumption on SOC influences on soil  
83 hydraulic properties were based on evidence from pedotransfer functions (PTFs). Feng et  
84 al. (2022) applied the crop model APSIM at a regional scale in China to model yield  
85 variability of maize and identified a statistically significant relationship between SOC and  
86 temperature-sensitivity of maize yields, suggesting that SOC contributes to climate  
87 resilience. A different model-based study design was implemented by Bonfante et al.  
88 (2020), who applied the SWAP model (Kroes et al., 2017) to 6 different Italian soils with  
89 assumed increased soil organic matter up to 2-4% in the topsoil. They found only minor  
90 increases in moisture supply capacity to be achieved with additional organic matter in the  
91 soil. In contrast to this, Ankenbauer and Loheide (2017), who applied a 1-D variably  
92 saturated groundwater flow model, found that increases in soil organic matter can

93 contribute as much as 88 mm to transpiration, or 35 additional water-stress free days,  
94 during a dry summer. Discrepancies in these studies' findings may be attributable to  
95 differences in pedo-climatic conditions as well as to model setups and the chosen levels  
96 and depths of SOC increase.

97 A systematic analysis of the impacts of SOC increase on drought stress reduction  
98 depending on depth of SOC increase is lacking so far. It is thus the aim of this study to  
99 systematically evaluate and quantify the potential benefits of increasing SOC for drought  
100 limitations in a regional context not only under current, but also under projected future  
101 climatic conditions. As a study case, we chose to evaluate how changes on SOC to  
102 different depths affect the drought stress experienced by maize at the Swiss Central  
103 Plateau region, where agricultural land use dominates and for which region climate  
104 projections suggest a decrease in summer precipitation and an increase in winter  
105 precipitation as climate change progresses (CH2018, Kotlarski and Rajczak (2018)).  
106 Annual precipitation sums are expected to remain largely the same over the projection  
107 period until the end of the century, ranging from 997 mm in the southwest to 1013 mm in  
108 the northeast. As previous studies have shown, drought stress is already limiting grain  
109 maize productivity under current conditions (Holzkämper et al., 2013; Holzkämper et al.,  
110 2015b) and this limitation is expected to become more significant as climate change  
111 progresses. According to Holzkämper (2020), irrigation demands for grain maize might  
112 increase by up to 20% by the end of this century, in comparison with the reference period  
113 of 1981-2000, assuming that the duration of the growth season remains constant. If late-  
114 maturing varieties would be grown, given the possibility of an extended growth season  
115 with increasing temperatures, irrigation water demand may even increase by 40%  
116 (Holzkämper, 2020). This raises concerns about the availability of irrigation water in the  
117 Swiss Central Plateau, where reoccurring irrigation bans have challenged farmers more

118 and more frequently in recent drought years (Bafu, 2019, 2016). Solutions to make Swiss  
119 production systems less reliant on supplementary irrigation are urgently needed.

120

121 **4. Data and methods**

122 To systematically evaluate the benefits of increasing soil organic carbon (SOC)  
123 for reducing drought limitations on a typical agricultural soil in the Swiss Central Plateau,  
124 we apply a field-scale agro-hydrological model that is deemed a suitable tool to interpret  
125 interactions between crops and the environment (Maharjan et al., 2018). The soil  
126 component of the model was parameterized using a recently developed pedo-transfer  
127 function and the model setup is validated against measurements of soil moisture dynamics  
128 in two lysimeters of a lysimeter station. Subsequently, the model is applied based on  
129 downscaled climate projection data in combination with scenarios of soil carbon  
130 increases.

131

132 **4.1 Agro-hydrological modelling with SWAP**

133 The Soil Water Atmosphere Plant model (SWAP, version 4.0.1) (Kroes et al.,  
134 2017) is a physically based agro-hydrological model that simulates the transport of water,  
135 solutes, and heat in the unsaturated (vadose) zone and optionally the upper part of the  
136 saturated (groundwater) zone with the upper boundary condition defined by atmospheric  
137 conditions. Major arable crops and grasslands can be explicitly simulated in SWAP via  
138 incorporation of the WOFOST (WOOrld FOod STudies, De Wit et al. (2019)) model or by  
139 using a simple crop module.

140 In interaction with the crop development, the model simulates the heat and solute  
 141 transport dynamics of variably saturated soils by employing the Richards equation in the  
 142 vertical direction, including a sink term for root water uptake:

$$C(h) \frac{\partial h}{\partial t} = \frac{\partial \left[ K(h) \frac{\partial(h+z)}{\partial z} \right]}{\partial z} - S_a(h) \quad [1]$$

143 where  $C(h)$  ( $\text{cm}^{-1}$ ) is the specific water capacity, the derivative of the soil water retention  
 144 function  $\theta(h)$ , which describes the relation between water content  $\theta$  ( $\text{cm}^3 \text{cm}^{-3}$ ) and soil  
 145 water suction  $h$  (cm, defined as positive at unsaturated conditions),  $t$  (d) is time,  $K(h)$   
 146 ( $\text{cm d}^{-1}$ ) is the hydraulic conductivity as a function of  $h$ ,  $z$  (cm) is the vertical spatial  
 147 coordinate (negative downwards), and  $S_a(h)$  ( $\text{d}^{-1}$ ) is a sink term representing the rate of  
 148 soil water extraction by plant roots.

149 The relationship  $\theta(h)$  and  $K(h)$  are defined by the van  
 150 Genuchten (1980) - Mualem (1976) (VGM) equations:

$$\theta(h) = \theta_r + \frac{(\theta_s - \theta_r)}{[1 - |\alpha h|^n]^m} \quad [2]$$

$$K(h) = K_s \theta^l \left[ 1 - \left( 1 - \theta^{\frac{1}{m}} \right)^m \right]^2$$

151 where  $\theta_s$  and  $\theta_r$  are the saturated and residual soil water content ( $\text{cm}^3 \text{cm}^{-3}$ ),  $\alpha$  ( $\text{cm}^{-1}$ ),  $n$ ,  $m$   
 152 ( $m = 1-1/n$ ), and  $l$  are empirical shape parameters,  $K_s$  is the saturated hydraulic  
 153 conductivity ( $\text{cm d}^{-1}$ ) and the relative degree of saturation,  $\theta$ , is expressed as  
 154  $\theta = (\theta - \theta_r)/(\theta_s - \theta_r)$ .

155 In our study, the model used crop properties and atmospheric conditions on a  
 156 daily basis to calculate the potential evapotranspiration based on the Penman-Monteith  
 157 equation. Water stress was evaluated according to the reduction function by Feddes  
 158 (1978), with the optimal root water uptake in the  $h$  ranges of -325.0 cm ( $h_{3H}$ ) or -600 cm

159 (h<sub>3L</sub>) to -30 cm (h<sub>2</sub>), oxygen stress linearly increasing for h higher than -15 cm (h<sub>1</sub>) and  
 160 drought stress linearly increasing for h smaller than -8000 cm (h<sub>4</sub>). The crop growth  
 161 module considers that the actual transpiration can be reduced by drought (too dry),  $\alpha_d(z)$ ,  
 162 lack of oxygen (too wet),  $\alpha_o(z)$ , or too saline conditions (physiological drought),  $\alpha_s(z)$ ,  
 163 which factors are known to reduce crop growth. The actual root water flux,  $S_a(z)$  (d<sup>-1</sup>), is  
 164 then a function of all considered stresses:

$$S_a(z) = \alpha_d(z)\alpha_o(z)\alpha_s(z)S_p(z) \quad [3]$$

165 where  $S_p(z)$  is the potential root water extraction rate at a certain depth. The actual  
 166 transpiration,  $T_a$  (cm d<sup>-1</sup>), is calculated by integrating the root water flux over the root  
 167 zone:

$$T_a = \int_{-D_{root}}^0 S_a(z) \partial z \quad [4]$$

168 where  $D_{root}$  is the root layer thickness (cm).

169 In our simulations, we did not consider stresses caused by saline conditions and  
 170 focused on the drought-induced transpiration reduction ( $T_{redry}$ ) as an indicator of  
 171 drought stress during the cropping period.

172 **4.2 Climate data of three distinct study sites from measured and projected**  
 173 **scenarios**

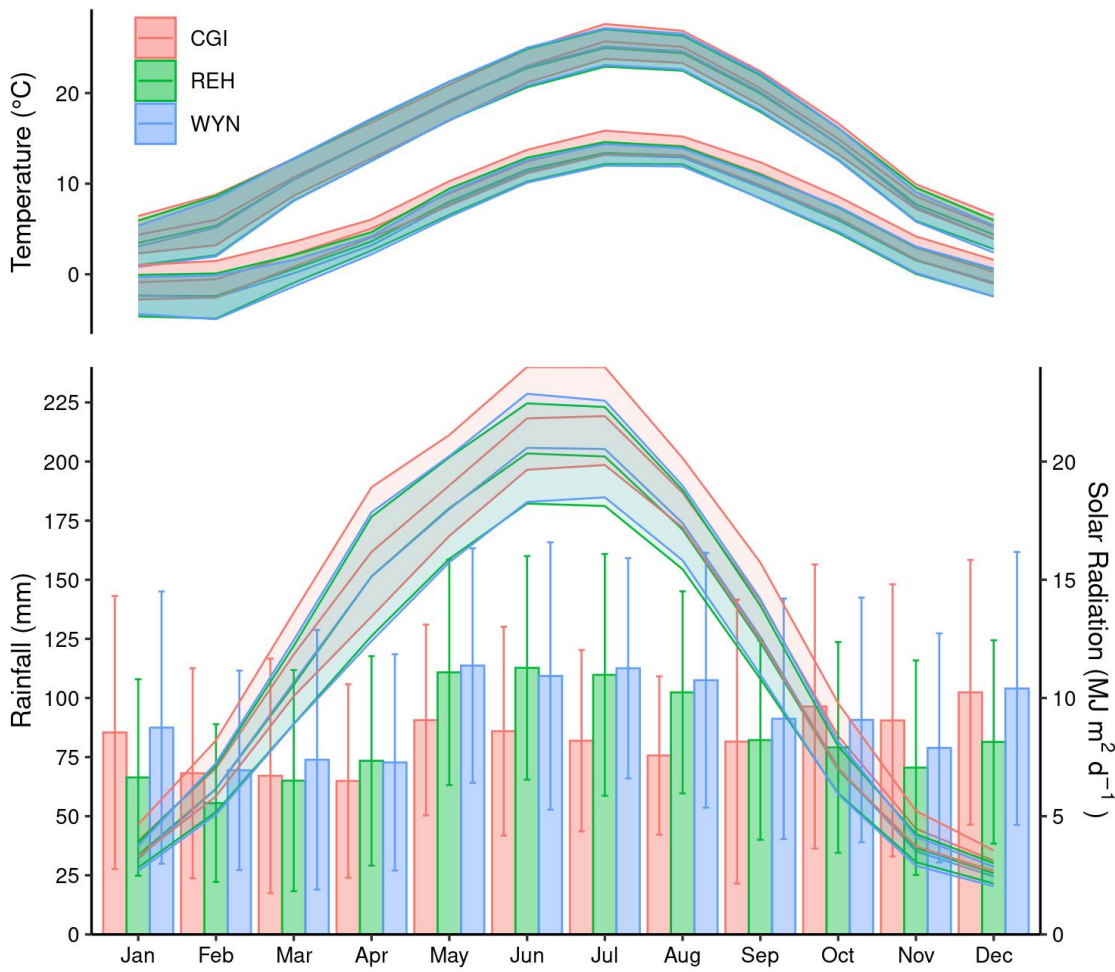
174 Typical Swiss agricultural conditions were evaluated at three distinct sites  
 175 distributed along the Swiss Central Plateau (the main agricultural production zone in  
 176 Switzerland): Nyon-Changins (CGI), Zürich-Reckenholz (REH), and Wynau (WYN).  
 177 Measured climatic variables from meteorological stations were obtained from  
 178 MeteoSwiss. Table 1 contains annual mean values of the meteorological variables  
 179 required by SWAP, while Figure 1 presents their seasonal variation. While the three sites

180 have similar altitude, on average, the CGI site has the driest and warmest climate, with  
 181 higher solar radiation and wind speed. WYN is on average the wettest and coldest. In all  
 182 sites the rainfall is relatively well distributed during the year, with higher precipitation,  
 183 temperature and solar radiation in the summer season.

184 Table 1 Site description and climatic variables based on mean  $\pm$  standard deviation values  
 185 observed between 1981 and 2022 from MeteoSwiss.

	Meteorological station		
	CGI (Changins)	REH (Reckenholz)	WYN (Wynau)
Altitude (m)	455	443	422
Latitude	46.4 N	47.4 N	47.3 N
Longitude	6.2 E	8.5 E	7.8 E
Rainfall (mm y <sup>-1</sup> )	997 $\pm$ 147	1013 $\pm$ 146	1117 $\pm$ 188
T <sub>min</sub> (°C)	6.5 $\pm$ 5.7	5.1 $\pm$ 5.9	5.0 $\pm$ 5.9
T <sub>max</sub> (°C)	14.8 $\pm$ 7.8	14.3 $\pm$ 8.0	14.3 $\pm$ 8.2
Solar radiation (MJ m <sup>2</sup> d <sup>-1</sup> )	12541.5 $\pm$ 7035.4	11372.0 $\pm$ 6738.6	11437.9 $\pm$ 6865.4
Vapour pressure (kPa)	0.98 $\pm$ 0.36	0.98 $\pm$ 0.38	0.99 $\pm$ 0.38
Wind speed (m s <sup>-1</sup> )	2.4 $\pm$ 0.2	1.8 $\pm$ 0.3	1.7 $\pm$ 0.3

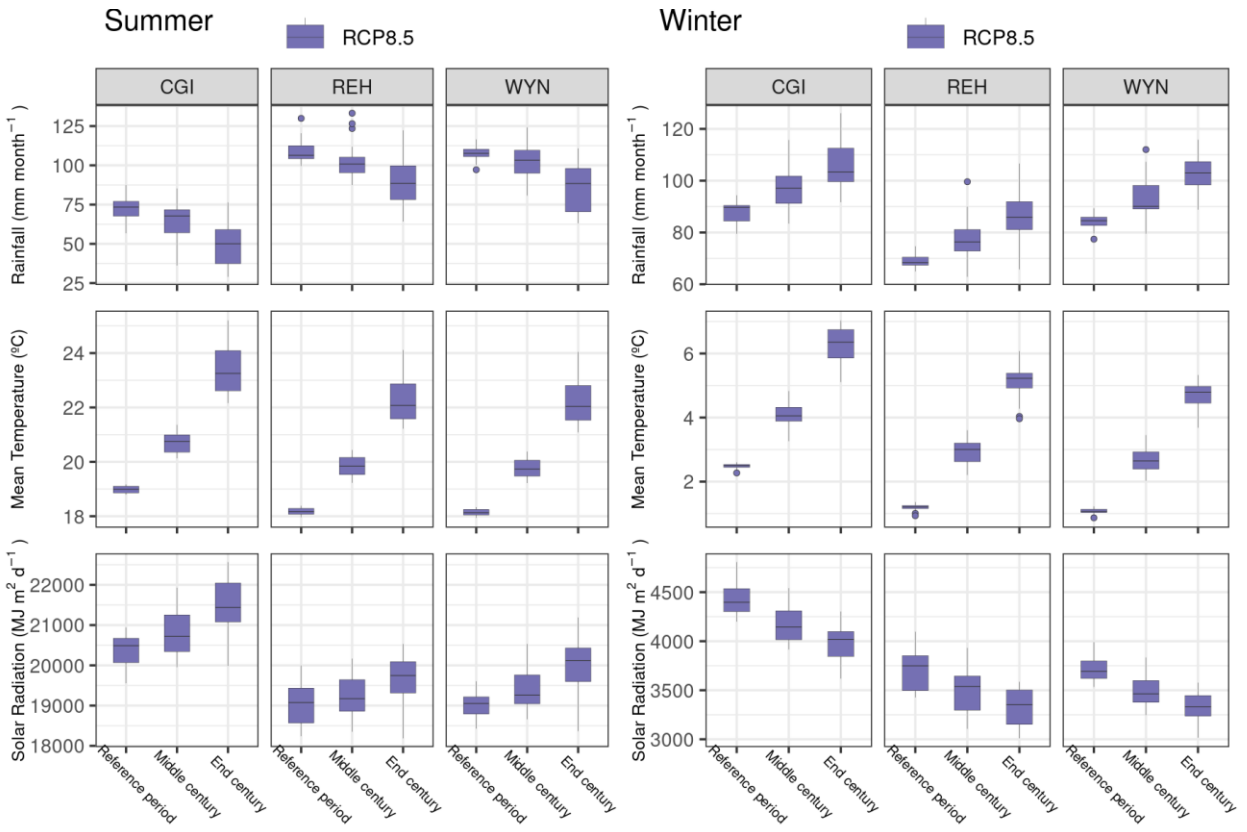
186



187 Figure 1 Seasonal variability of climatic variables considering monthly mean  $\pm$  standard  
 188 deviation (shades and bars) values observed at the meteorological stations between 1981  
 189 and 2022. Rainfall corresponds to monthly sums, while other variables represent daily  
 190 values averaged by month. Minimum (bottom lines) and maximum (upper lines)  
 191 temperatures are presented.

192  
 193 Future scenarios were evaluated using climate projections developed by the  
 194 National Centre for Climate Services (NCCS) in Switzerland (Kotlarski and Rajczak,  
 195 2018). The dataset contains transient daily time series for the period 1981-2099 for several  
 196 variables at individual Swiss stations (DAILY-LOCAL), produced by applying a  
 197 statistical downscaling and bias-correction method (Quantile Mapping, QM) to the  
 198 original output of all EURO-CORDEX climate model simulations employed in CH2018  
 199 (Kotlarski and Rajczak, 2018). From all available projections with different  
 200

201 Representative Concentration Pathways (RCP), we selected the ones that presented the  
202 dataset with all required input variables for SWAP, as listed in [Table 1](#). In total, we used  
203 22 projections for RCP8.5, 17 for RCP4.5, and 8 for RCP2.6. For more details about  
204 selected model chains, see Supplementary Material (Section S1). [Figure 2](#) presents an  
205 overview of the projected climate variables for the summer (JJA) and winter (DJF)  
206 months during the baseline (1981-2020), mid-century (2031-2060) and end-of-century  
207 (2081-2099) periods for each of the RCP8.5. More details about the other RCPs as  
208 Supplementary Material (Section S2). With the most pessimistic assumption about the  
209 evolution of greenhouse gas emissions (RCP8.5), climate projections estimate lower  
210 precipitation, higher temperature and higher solar radiation for future summers, while  
211 they predict higher precipitation, higher temperature and lower solar radiation for winters  
212 at the end of the century.



213

214 Figure 2 Summary of climatic variables considering monthly mean values at the stations  
 215 Changins (CGI), Reckenholz (REH), and Wynau (WYN) for the projections RCP8.5.  
 216 Summer was considered as the months June, July and August, winter corresponds to  
 217 December, January and February. Reference period: 1981-2020, mid-century: 2031-  
 218 2060, end-of-century: 2071-2099. Rainfall corresponds to monthly sums, mean  
 219 temperature is the mean between maximum and minimum temperature per day, averaged  
 220 by month, solar radiation corresponds to daily values averaged by month.

221        **4.3      Model reference data and setup**

222              Reference information on soil water dynamics at four different depths (10, 30,  
223        60, and 90 cm) were available from lysimeters of 135cm depth and 1m<sup>2</sup> surface area at  
224        the lysimeter facility of Agroscope Zürich-Reckenholz (Prasuhn et al., 2016). Soil  
225        moisture was monitored from 2009 to 2022 using frequency domain reflectometry sensors  
226        (FDR; ThetaProbe ML2x, Delta-T Devices) at the depths of 10, 30, 60, and 90 cm. In  
227        each of the lysimeters two identical sensors were installed at each depth with a time  
228        resolution of one hour. We utilize the data of two lysimeters that contain similar soil  
229        monoliths from a typical agricultural soil nearby (Loamy-silty Cambisol above ground  
230        moraine (Fao, 2015), see [Table 2](#) for the soil profile description). The monoliths have a  
231        15 cm layer of purified quartz sand and gravel at the bottom that help facilitate free  
232        drainage.

233              For the model setup, the measured physical and chemical soil parameters ([Table](#)  
234        [2](#)) were used in combination with the pedotransfer function (PTF) developed by Szabó et  
235        al. (2021), using the R package in which the euptfv2 is implemented (Weber et al., 2020).  
236        The euptfv2 is a Random Forest-based PTF with various options for inputs and output  
237        parameters, and has proven to be one of the most accurate PTFs to estimate soil hydraulic  
238        properties for Europe when tested on diverse datasets (Nasta et al., 2021). As the standard  
239        setup for all simulations, we used option ‘PTF02’, which requires the depth of the soil  
240        layer, soil texture, and soil organic carbon content (SOC) as input, and estimates the VGM  
241        parameters for the soil water retention [ $\theta(h)$ ] and hydraulic conductivity [ $K(h)$ ] functions  
242        (Eq. [\[2\]](#)).

243

244

245 Table 2 Soil physical and chemical properties of the evaluated typical Swiss agricultural  
 246 profile at the Lysimeter facility at Agroscope Reckenholz. SOC: soil organic carbon, BD:  
 247 bulk density, PD: particle density, CEC: cation exchange capacity. Soil class and horizon  
 248 description according to Prasuhn et al. (2016).

Horizon	Depth cm	Clay %	Silt %	Sand %	SOC %	BD g cm <sup>-3</sup>	pH <sub>H<sub>2</sub>O</sub>	pH <sub>CaCl<sub>2</sub></sub>	PD g cm <sup>-3</sup>	CaCO <sub>3</sub> %	CEC cmol+ kg <sup>-1</sup>
Ahp	0-25	25	50	25	1.48	1.36	6.8	6.4	2.63	0.1	16.2
Abcn	25-32	24	54	22	1.09	1.44	7.1	6.6	2.68	0.2	15.67
Bcn(g)(x)	32-65	31	50	19	0.43	1.44	7.2	6.5	2.7	0.1	17.61
Bg	65-85	33	46	21	0.32	1.44	7.5	6.6	2.7	0.1	18.77
BCg	85-105	19	61	20	0.10	1.39	8.6	7.7	2.7	40.2	10.93
Cg	105-135	18	65	17	0.02	1.61	8.6	7.8	2.71	54.4	7.49

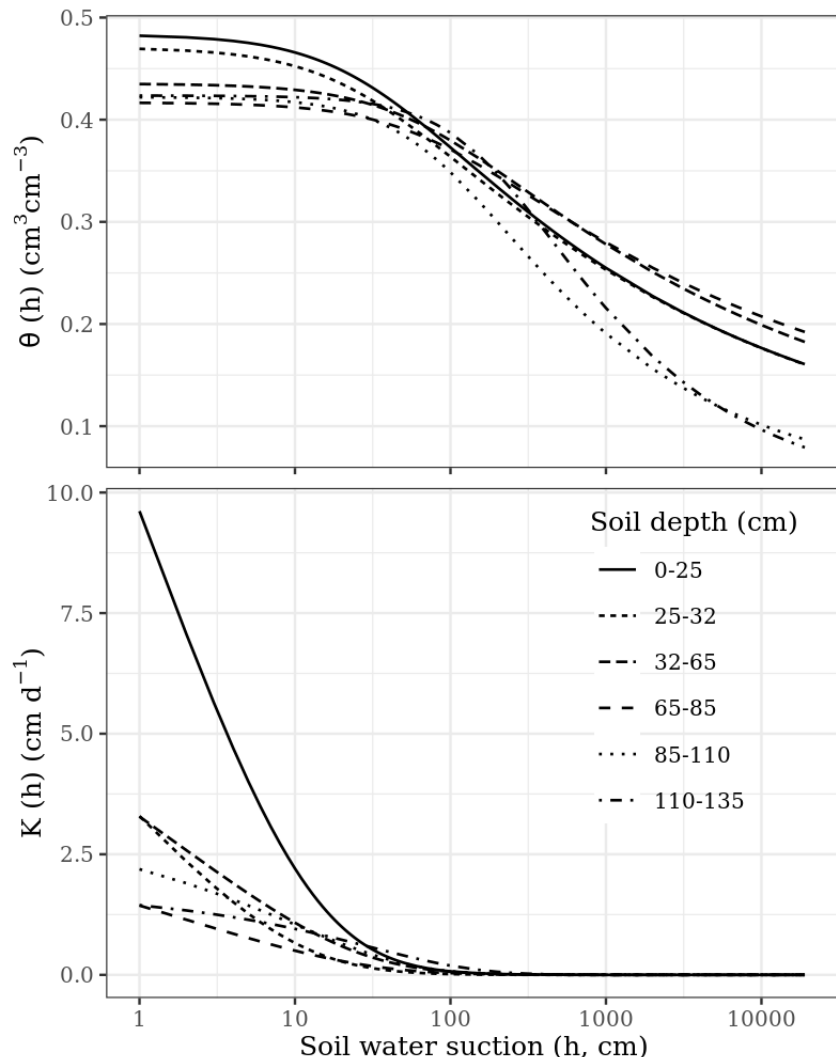
249

250 [Table 3](#) presents the parameters of Eq. [\[2\]](#) at the evaluated soil profile from the  
 251 Lysimeter station, calculated using the chosen PTF. The soil water retention and hydraulic  
 252 conductivity curves are visualized in [Figure 3](#).

253 Table 3 Soil hydraulic parameters calculated using the euptfv2 at the original soil profile,  
 254 considering option ‘PTF02’ that uses soil texture, soil carbon content and soil depth as  
 255 input.

Soil	Layer	Depth cm	$\theta_r$ cm <sup>3</sup> cm <sup>-3</sup>	$\theta_s$ cm <sup>3</sup> cm <sup>-3</sup>	$\alpha$ cm <sup>-1</sup>	n -	K <sub>s</sub> cm d <sup>-1</sup>	l -
Reckenholz	1	0-25	0.053	0.483	0.034	1.215	35.61	-1.59
	2	25-32	0.038	0.471	0.037	1.193	14.78	-0.70
	3	32-65	0.059	0.435	0.015	1.196	10.41	-0.62
	4	65-85	0.078	0.417	0.014	1.196	4.41	-1.23
	5	85-105	0.034	0.422	0.011	1.370	3.34	0.23
	6	105-135	0.026	0.424	0.005	1.441	1.77	0.09

256



257

258 Figure 3 Soil water retention ( $\theta$ ) and soil hydraulic conductivity (K) as function of the  
 259 soil water suction (h) at the evaluated soil profile estimated by the euptfv2 (option  
 260 'PTF02').

261 The validation of SWAP with the lysimeter information included three cropping  
 262 periods with grain or silage maize in 2009, 2015 and 2020, with annual precipitation of  
 263 1018.9, 831.5 and 855.2 cm, respectively. Daily time step was adopted and vertically, the  
 264 top soil layer up to 65 cm was discretized using 1.0 cm sub-compartments, while  
 265 subsequent layers were discretized with 5 and 10 cm sub-compartments. The boundary  
 266 condition was set to 'free outflow at soil-air interface', which is considered as a valid  
 267 option for lysimeters. The evapotranspiration was calculated using weather data and  
 268 application of the Penman-Monteith equation. No macropore flow, lateral drainage or

269 solute dispersion was simulated. For the validation, the daily averaged values of measured  
270 soil water content at each replicate sensor and depth (eight time series per lysimeter) were  
271 compared to the modeled values by SWAP. As validation metrics, we used the root mean  
272 square error (RMSE) and the Pearson correlation ( $r$ ). See Supplementary Material S3 for  
273 details on model setup.

274 **4.4 Design of simulation experiments**

275 In the absence of consistent and comparable data from long term and holistic  
276 studies that account for the impacts of management on soil hydraulic properties,  
277 pedotransfer functions (PTFs) are seen as a suitable choice to systematically account for  
278 linkages between SOC and soil hydraulic properties. We thus used the chosen PTF to  
279 systematically capture secondary effects of SOC instead of directly inferring the effects  
280 of specific drivers of change on the soil hydraulic properties due to the uncertain  
281 interaction effects between SOC, soil type, climate and management.

282 We assumed that management improvements have led to increased SOC from  
283 the beginning of the simulation period and that SOC remained stable over the simulation  
284 period, thereby testing different scenarios of successful carbon sequestration. The model  
285 parametrization included three distinct depth scenarios: i) changes in SOC occur only  
286 within the top 0-25 cm, ii) changes in SOC occur to 0-65 cm depth and, iii) changes in  
287 SOC are achieved for the entire soil profile. In terms of SOC change, we simulated the  
288 addition of up to 4% SOC to current SOC levels by 1% increments in the (i) and (ii) depth  
289 scenarios, but applied reduction factors of 0.8 and 0.6 for the 65-105 cm and 105-135 cm  
290 depths respectively in depth scenario (iii). This approach considers that obtaining greater  
291 SOC via management likely affects the topsoil more than the deeper soil layers. The  
292 outlined depth and SOC level scenarios are listed in Table 4 for easier comprehension.

293 It should be emphasized that the levels of SOC in the soil are dependent on  
 294 several factors including land use and management, climate, geomorphology, which were  
 295 considered as empirical relationships in this work.

296 Table 4 Description of %SOC levels added per depth and final values of SOC considering  
 297 the described scenarios i), ii), and iii). Shaded values represent the layers where changes  
 298 on SOC were applied.

Scenario	Soil depth (cm)	SOC added (%)	Effective depth of changes (cm)		
			i) 0-25	ii) 0-65	iii) 0 -135
0%	0-25	0	1.48	1.48	1.48
	25-32	0	1.09	1.09	1.09
	32-65	0	0.43	0.43	0.43
	65-85	0	0.32	0.32	0.32
	85-105	0	0.10	0.10	0.10
	105-135	0	0.02	0.02	0.02
1%	0-25	1	2.48	2.48	2.48
	25-32	1	1.09	2.09	2.09
	32-65	1	0.43	1.43	1.43
	65-85	0.8	0.32	0.32	1.12
	85-105	0.8	0.10	0.10	0.90
	105-135	0.6	0.02	0.02	0.62
2%	0-25	2	3.48	3.48	3.48
	25-32	2	1.09	3.09	3.09
	32-65	2	0.43	2.43	2.43
	65-85	1.6	0.32	0.32	1.92
	85-105	1.6	0.10	0.10	1.7
	105-135	1.2	0.02	0.02	1.22
3%	0-25	3	4.48	4.48	4.48
	25-32	3	1.09	4.09	4.09
	32-65	3	0.43	3.43	3.43
	65-85	2.4	0.32	0.32	2.72
	85-105	2.4	0.10	0.10	2.5
	105-135	1.8	0.02	0.02	1.82
4%	0-25	4	5.48	5.48	5.48
	25-32	4	1.09	5.09	5.09
	32-65	4	0.43	4.43	4.43
	65-85	3.2	0.32	0.32	3.52
	85-105	3.2	0.10	0.10	3.3
	105-135	2.4	0.02	0.02	2.42

299

300 To quantify the impacts of increasing SOC on drought stress in maize under  
301 climate change, SWAP was applied to the 22 climate projections at the three sites  
302 Changins (CGI), Reckenholz (REH), and Wynau (WYN) in combination with the  
303 scenarios of SOC increase listed in Table 4. We assumed grain maize to be sown on 6<sup>th</sup>  
304 May (DOY 126) and harvested on 17<sup>th</sup> Oct (DOY 290) as registered in the Swiss variety  
305 trial data for a medium-late variety type (Agroscope, 2023). The bottom boundary  
306 condition was set as free drainage, representing a soil profile with deep groundwater  
307 levels. For details of general SWAP parameterization see Supplementary Material S3.

308 All simulations considered rain fed conditions and were performed using the  
309 simple crop growth module for a static crop, which simulates a fixed development of leaf  
310 area index and rooting depth, independent of climatic conditions, in order to keep the  
311 cropping period fixed for all scenarios. In this study we worked with 165 days of crop  
312 growing period; the crop component's parameterization is described in Supplementary  
313 Material S4.

314 Overall, we conducted a total of 990 simulation runs (5 levels of SOC  $\times$  3 soil  
315 depths  $\times$  3 sites  $\times$  22 climate projections) for the period 1981-2099, and used cumulative  
316 amounts of drought-induced transpiration reduction ( $T_{redry}$ ) as an indicator of drought  
317 stress during the cropping period. The 10-year moving average of  $T_{redry}$  was calculated  
318 to represent decadal changes and exclude interannual variability. The range of  $T_{redry}$   
319 values among the available climate projections were represented by the 0.05 quantile  
320 ( $q_{0.05}$ ) and the 0.95 quantile ( $q_{0.95}$ ) as upper and bottom boundaries, respectively. The  
321 difference between management scenarios in terms of crop transpiration, defined as the  
322 average transpiration gain (ATG) with SOC increase, was calculated as the difference  
323 between the scenario with no addition of SOC (0%) and the one with the maximum  
324 addition of SOC (4%).

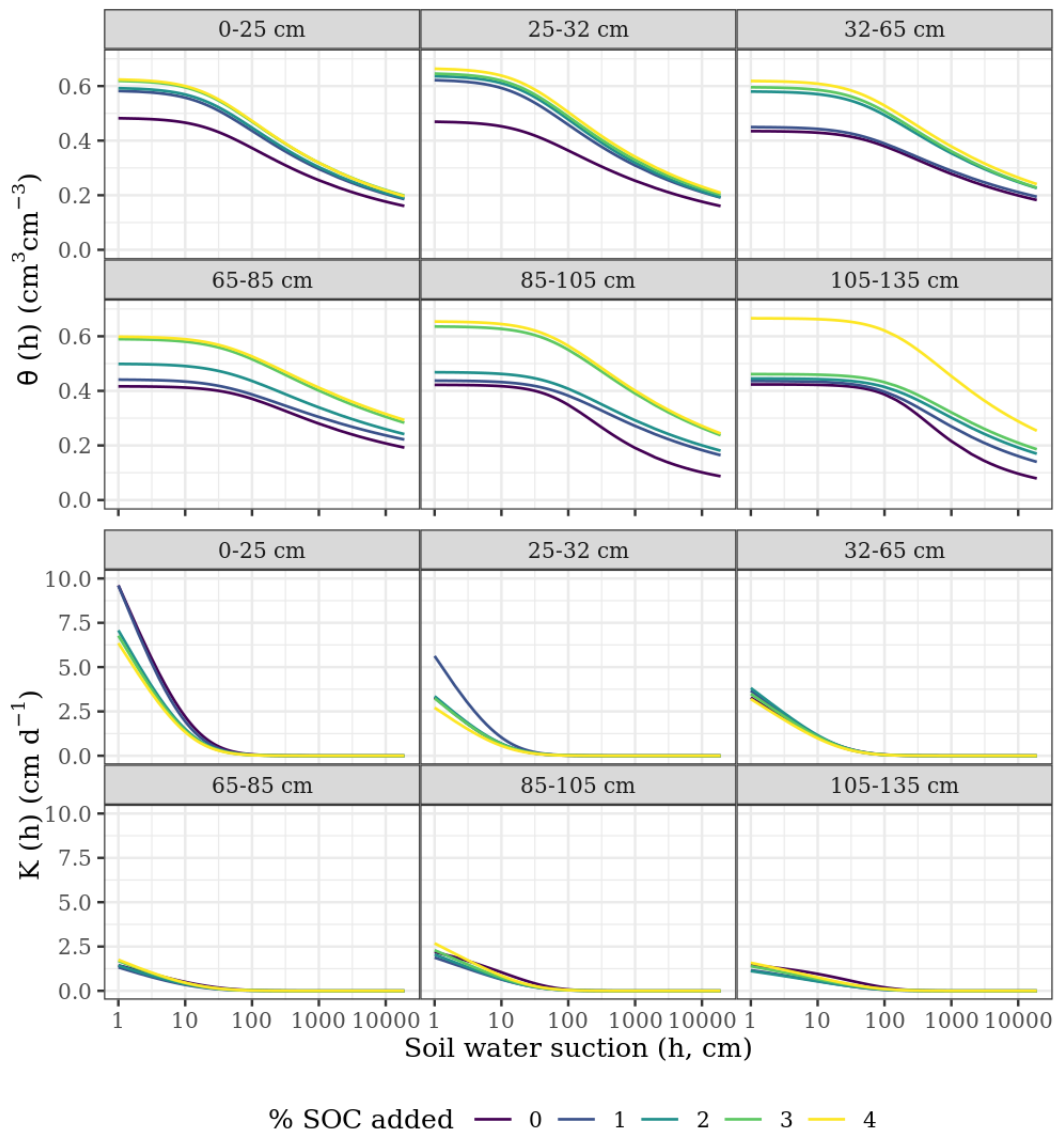
325 **5. Results**326 **5.1 Model validation**

327       Using the soil hydraulic parameters from [Table 3](#), we simulated soil water  
 328 content in the lysimeter soil profiles and compared them with moisture data measured by  
 329 FDR sensors. The lumped values of the two lysimeters, considering all maize cropping  
 330 periods (2009, 2015, and 2020), all depths (10, 30, 60, and 90 cm) with duplicated  
 331 sensors, resulted in a median ( $q_{0.5}$ ) RMSE of  $0.066 \text{ cm}^3 \text{ cm}^{-3}$  ( $q_{0.05}=0.050 \text{ cm}^3 \text{ cm}^{-3}$ ,  
 332  $q_{0.75}=0.098$ ) and correlation median correlation  $r$  of 0.79 ( $q_{0.05}=0.68$ ,  $q_{0.75}=0.84$ ). In  
 333 general, the simulations were more accurate for the deeper layers as compared to the  
 334 topsoil. At 10 cm, the RMSE was on average  $0.11 \text{ cm}^3 \text{ cm}^{-3}$ , whereas it was  $0.04 \text{ cm}^3 \text{ cm}^{-3}$   
 335 at the bottom.

336

337 **5.2 Effect of increasing SOC on the soil hydraulic properties and soil water  
 338 balance**

339       The effects of adding different amounts of SOC at different soil layers ([Figure](#)  
 340 [4](#)) are reflected in PTF estimates of soil hydraulic properties with updated SOC contents.  
 341 The “0%” line, corresponding to the VGM parameters in [Table 3](#), represent the properties  
 342 of the different soil layers with current SOC. For the soil water retention curve, the effects  
 343 of the increase in SOC reflected an estimated increase in pore space, whose expression  
 344 varied with soil depth and added SOC. In the topsoil, the differences between the addition  
 345 of 1% and 4% SOC were not as remarkable as in the subsoil layers, where an addition of  
 346 1% SOC lead to a substantial increase in estimated pore space. For saturated hydraulic  
 347 conductivity, the overall trend was a reduction in conductivity with the increase in SOC,  
 348 with the biggest contrasts found in the topsoil.

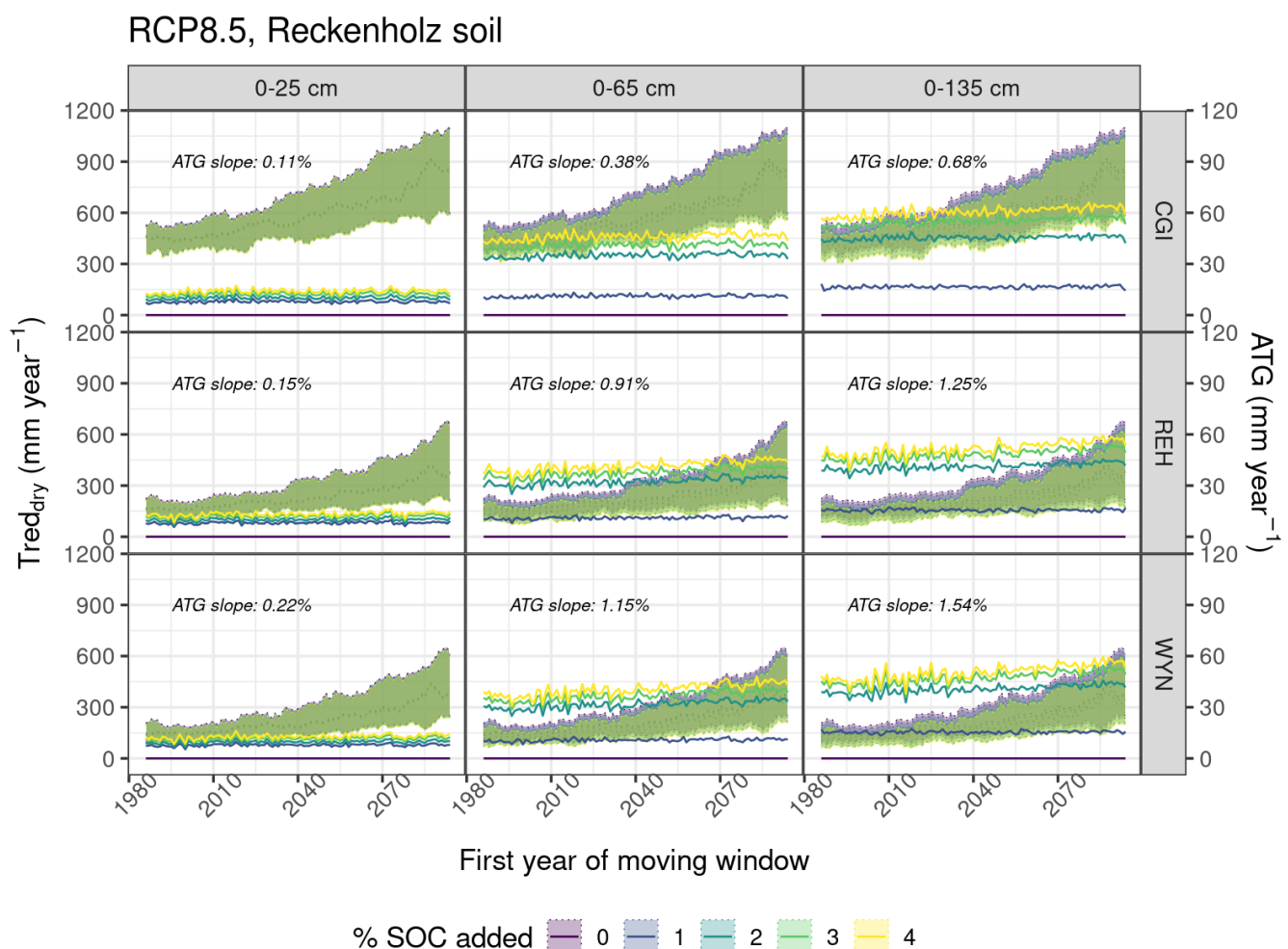


349

350    Figure 4 Effects of SOC increase on the soil water retention ( $\theta$ ) and soil hydraulic  
 351    conductivity ( $K$ ) as function of the soil water suction ( $h$ ) as predicted by euptfv2, option  
 352    'PTF02'.

353    Considering effects of adding SOC at different soil depths, Figure 5 presents an  
 354    overview of the transient simulations between 1980 and 2099 with the most unfavorable  
 355    climate scenario projections (RCP8.5). For each year of simulation, a range of values of  
 356     $T_{redry}$  was generated by the 22 climate projections, which are being represented by a  
 357    band defined by the lines  $q_{0.05}$  and  $q_{0.95}$  quantiles, and the  $q_{0.5}$  quantile (median) is  
 358    represented by a line within that band. The average transpiration gain (ATG) line is the  
 359    difference between the median ( $q_{0.5}$ ) values of the original Reckenholz soil profile (i.e.

360 0% SOC addition) and the one that had 4% SOC added. The ATG can be interpreted as  
 361 the amount of seasonal transpiration gained in response to increased SOC. The absolute  
 362 increase in  $T_{redry}$  comparing the reference period with the end of the century was on  
 363 average 269, 207, and 269 mm at CGI, REH and WYN, respectively. Additional results  
 364 considering other Representative Climate Projections (RCP 2.6 and 4.5) are presented in  
 365 the Supplementary Material (Section S5).



366

367 Figure 5 Transpiration reduction due to drought stress ( $T_{redry}$ ) (left axis, green band) for  
 368 actual and future climate conditions considering different levels of SOC increase in the  
 369 soil at different effective soil depths; and average transpiration gain, ATG, (right axis,  
 370 colored lines) between 0 and 4% addition of SOC. Climate projections considered the  
 371 RCP8.5 pathway and were averaged for every 10 years. The green shaded area of  $T_{redry}$   
 372 refers to the values between (dotted) quantiles  $q_{0.05}$  and  $q_{0.95}$  of the climate projections.  
 373 ATG is interpretable as average seasonal gain in transpiration due to SOC increase, and  
 374 ATG slope refers to the slope of the ATG line between 0 and 4% SOC addition.

375

376 According to the simulated scenarios, the main driver of the absolute values of  
 377  $T_{redry}$  is the climate, with more drought stress under the climate of the drier site (CGI)  
 378 and very similar stress levels under the climate of the other two sites, REH and WYN,  
 379 that are wetter and appear to be somewhat resembling. There was a clear tendency of  
 380 increased stress towards the end of the century, driven by more unfavorable climatic  
 381 conditions during the cropping period (Figure 2). The ATGs were very similar amongst  
 382 the three considered climates, with maximum values around  $60 \text{ mm year}^{-1}$ , and slightly  
 383 higher in the CGI climate. The ATG slopes calculated between the beginning and the end  
 384 of the century were higher at REH and WYN, which are the sites with less water stress  
 385 under current conditions. This is an implication of not considering a gradual build-up  
 386 period for increased SOC, but considering the same levels of SOC addition for the entire  
 387 simulation period.

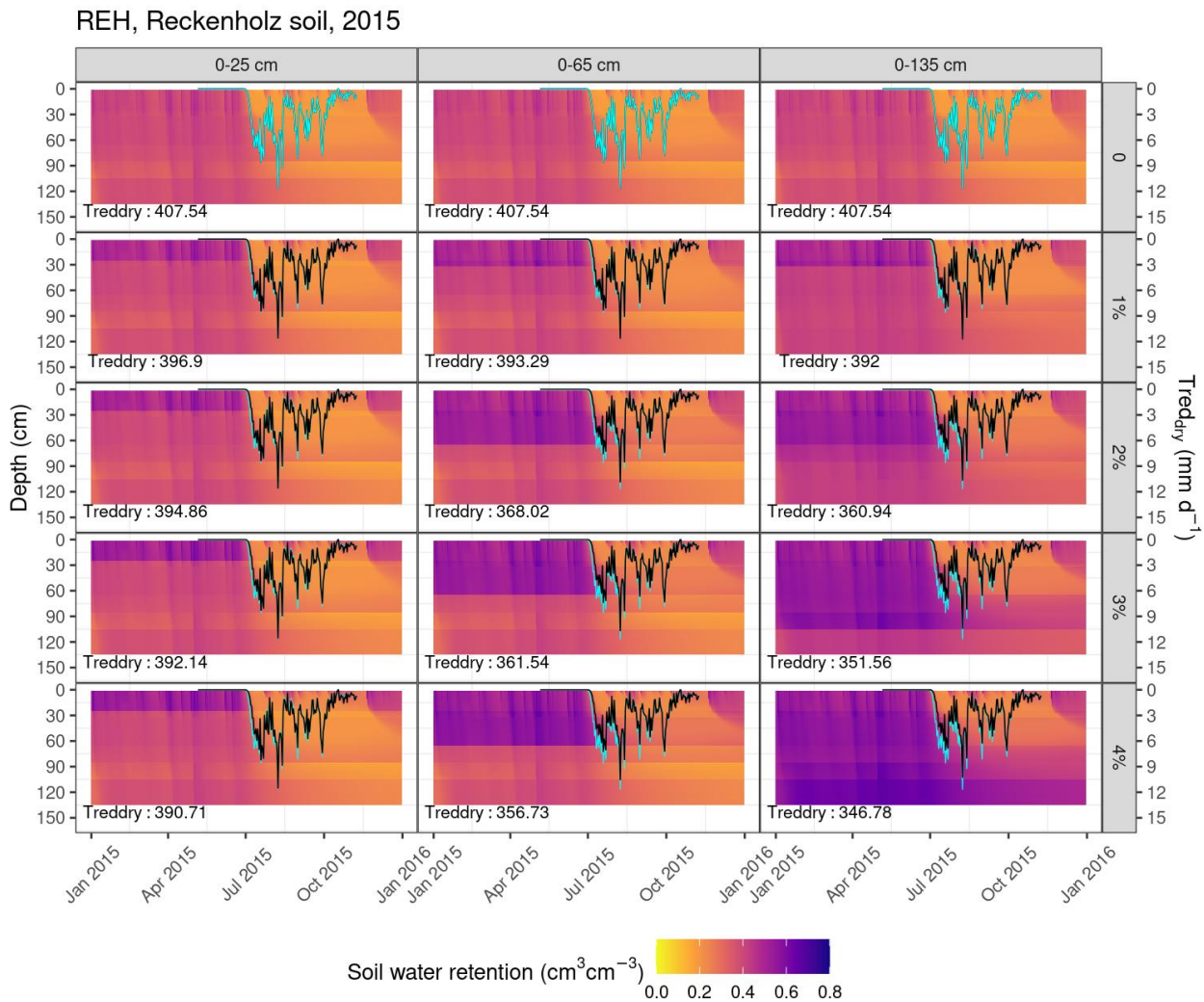
388 The simulations were performed considering the addition of SOC down to three  
 389 different depths (25, 65, and 135 cm). The addition of SOC to the top 25 cm seems to  
 390 have a modest effect on  $T_{redry}$ . The effects of increasing SOC all the way to 135 cm are  
 391 the greatest, but are comparable to the intermediate option of adding SOC till 65 cm  
 392 depth. In general, adding 2% SOC already lead to considerable reduction in  $T_{redry}$ , and  
 393 is a more realistic, easier-to-implement alternative to adding 4% SOC.

394

395 **5.3 Detailed soil water dynamics and drought stress over the cropping  
 396 period**

397 Figure 6 depicts, as an example, how the soil moisture profile develops and how  
 398 the ATG in moisture deficit builds up during the simulated 2015 cropping year at the REH

399 site, with the different increased SOC levels in the entire soil profile (depth scenario iii).  
400 The addition of SOC leads to a clear pattern of increasing soil water retention.. The blue  
401 line depicts the daily simulated crop transpiration deficit ( $T_{redry}$ ) of the 0% added SOC  
402 scenario, while the black lines depict the same obtained for the relevant depth and SOC  
403 addition scenario in each plot. Their difference, when cumulated for the year, yields the  
404 transpiration deficit ATG for the given year and scenario. The most remarkable seasonal  
405 ATGs were observed in the beginning of the cropping season, and could be linked to  
406 increased soil water retention capacity combined with the availability of water in that  
407 season. According to Figure 4, increased SOC content generally yielded increased soil  
408 water retention capacity relative to the base scenario of no SOC addition. In the early  
409 cropping season this increased capacity is capitalized on in the form of retaining more  
410 water in the system by the end of the recharge-period in the wet and cold winter and spring  
411 season. The simulated extra amount of water is clearly demonstrated in Figure 6. During  
412 the early part of the growing season, this excess water then becomes available to the crop,  
413 dampening the effects of any drought-stress, or at least delaying its onset. The soil will  
414 also not dry out to the same degree during the later half of the season, or at least not to  
415 the same depth. Similar results for the other evaluated sites are presented in the  
416 Supplementary Material (Section S6).



417

418 Figure 6 Detailed profile of soil water content (left axis)  
 419 and Treddry (right axis, black lines)  
 420 according to the different added SOC levels at the Reckenholz site (REH) in the  
 421 year of 2015. The blue line represents Treddry for the original soil profile (0% SOC).  
 422 When cumulated for the year, their difference yields the annual ATG in crop transpiration  
 deficit that is due to the addition of carbon to the soil.

423 **6. Discussion**424 **6.1 Increasing soil organic carbon reduces drought stress in maize**

425 We observed that according to the predictions of the used PTF, an increase of  
426 SOC has a small effect on, but generally decreases soil hydraulic conductivity ([Figure 4](#)).  
427 This may be counter-intuitive in that textbook knowledge connects greater SOC content  
428 with better soil structure formation, greater porosity, and in turn to enhanced water  
429 transport properties (hydraulic conductivity) (Nemes et al., 2005). However, several  
430 studies have now emerged that correlated greater SOC content with lower hydraulic  
431 conductivity. These studies include both experimental data and the mining of several  
432 extended databases using machine-learning (Nemes et al., 2005; Wang et al., 2009; Jarvis  
433 et al., 2013; Larsbo et al., 2016). The rationale behind this notion is that when SOC  
434 content increases, there is enhanced porosity, but the tortuosity of conductive pathways  
435 may increase due to enhanced microbial activity and the formation of more complex  
436 aggregates, resulting in better water retention but reduced hydraulic conductivity. Some  
437 of these authors noted increased predicted water retention in the effective porosity (i.e.  
438 the range between field capacity and saturation), which supports the proposed notion.

439 Results from this simulation study suggest that increases in SOC would generally  
440 decrease drought stress in maize cultivated on a typical agricultural soil in Switzerland.  
441 The summer season precipitation amount at the evaluated sites is expected to be decreased  
442 by around 60-65 mm till the end of the century ([Figure 2](#)). In this scenario, a 2% addition  
443 of SOC can reduce drought stress of maize by 10.5 to 40 mm during the cropping season  
444 and potentially compensate part of the rainfall reduction with climate change. Bonfante  
445 et al. (2020) suggests that the effect of SOC on moisture supply capacity should be  
446 evaluated in more climatic zones in order to obtain a broader picture of its potential

447 impact. What we observed in this work was that the degree of decrease in  $T_{redry}$  was  
448 only minimally dependent on regional climatic conditions, with the wettest site (WYN)  
449 benefitting least from the SOC increases under current climate conditions. As conditions  
450 get drier, as projected with climate change for the Swiss Central Plateau, the transpiration  
451 gain increases, but reaches a maximum at 60 mm with SOC increase down to 135 cm.

452 Our study suggests minor benefits of increasing SOC in the topsoil (maximum  
453 ATG reached is 15 mm, Figure 5). However, if SOC was increased down to at least  
454 65 cm, this beneficial effect can be considerably higher (maximum ATG reached is  
455 45 mm, Figure 5). Overall, the maximum ATG of  $T_{redry}$  quantified in this study was  
456 60 mm (at the end of the century, with SOC increase down to 135 cm), suggesting that  
457 without supplementary irrigation, seasonal crop transpiration can be up to 60 mm greater  
458 with increased SOC, compared to the reference situation. This amount is comparable to  
459 1-2 irrigation dosages and makes up for roughly 30% of the average theoretical irrigation  
460 water demand estimated by Holzkämper (2020) for the region between Wynau (WYN)  
461 and Changins (CGI). The productivity gain to be achieved will strongly depend on the  
462 period in the cropping cycle when this extra water will be available. Considering that  
463 transpiration benefits are greatest at the onset of drought during early summer (Figure 6),  
464 the productivity gains may be particularly high if the effect coincides with the critical  
465 reproductive phase of the crop. This might imply that transpiration gains achieved with  
466 increases in SOC have a significant potential to increase yield stability, particularly in  
467 situations where and when irrigation is not an option.

468 The positive slopes of calculated ATGs of  $T_{redry}$  (i.e. transpiration gained with  
469 SOC increase) in Figure 5 suggest that the benefits of SOC additions could slightly  
470 increase with projected future climate change – especially at WYN, the least water-  
471 limited site under current conditions. At the driest site, CGI, the ATG (i.e. benefit of SOC

472 increase) reached under current climatic conditions is roughly at the same level as it is at  
473 WYN at the end of the century. These findings imply that the benefits of SOC  
474 accumulation may increase as water input (precipitation) during the cropping period  
475 decreases over time. However, there appears to be a threshold beyond which benefits are  
476 not seen as  $T_{red, dry}$  further increases (the *ATG slope* in Figure 5 decreases from the wettest  
477 to the driest site). The benefit of “extra water availability” comes from the balance of two  
478 elements: available water and available storage capacity. It appears that the available  
479 storage capacity component is enhanced by the addition of some SOC (i.e. 2% addition  
480 in our simulations), but the system becomes water-limited by the end of the century. The  
481 extra storage capacity that additional SOC may yield will not be filled up by the actual  
482 water input, and the potential extra benefit cannot be realized. The within-year occurrence  
483 of the same phenomenon is observable in [Figure 6](#). The biggest reduction in  $T_{red, dry}$  occurs  
484 in the beginning of the cropping season, when the increased retention capacity was present  
485 at the same time when ample amount of water was recharging the system during and after  
486 the cold, rainy season, with little or no plant water uptake.

487 A similar balance is likely to apply when the outcome of a 135 cm deep  
488 application of added SOC is interpreted. When simulating SOC addition to 135 cm depth  
489 vs. only 65 cm, the added benefit in terms of reduced crop  $T_{red, dry}$  appears to be limited.  
490 We argue that while some excess water storage capacity is simulated, there is little actual  
491 benefit realized from that, given the reduced amount of predicted precipitation by the end  
492 of the century. In addition, few, if any, crop roots reach that depth, which means that the  
493 only way the crop has direct benefit from water stored in the deeper soil layers in the  
494 growing season is if water redistributed upwards via capillary and vapor transport.

495

496      **6.2      Possibilities to increase soil organic carbon**

497      Results from our study suggest that the beneficial effects of increasing SOC are  
 498      small if SOC is only increased in the top-soil (0-25 cm), but become more significant if  
 499      SOC is increased to only 65 cm depth by at least 2%. We assumed that such SOC  
 500      increases can be achieved, while different management adaptations and combinations  
 501      thereof may be suitable to reach this target. Commonly considered strategies to increase  
 502      SOC include additions of organic amendments, planting of deep-rooting crops, cover-  
 503      cropping, intercropping, mulching with organic material, retaining crop residues in the  
 504      field and reduced tillage or no-till (Topa et al., 2021; Ipcc, 2019). No-till or reduced tillage  
 505      decreases the carbon oxidation process and soil disturbance with the loss of soil organic  
 506      carbon and nutrient availability (Modak et al., 2019; Kan et al., 2020). Also, Angers and  
 507      Eriksen-Hamel (2008) found that tillage affects the distribution of SOC over the depth of  
 508      the soil profile with important implications in crop water availability. A meta-analysis on  
 509      effects of tillage on SOC (Krauss et al., 2022) has shown that it is not uncommon that  
 510      depletion in SOC of a subsoil layer co-occurs with increased SOC levels in the topsoil.  
 511      We tested this with the particular soil and PTF used in our study, and found that the  
 512      hydrological effects of reducing SOC at the depth of 25-32 cm were almost identical to  
 513      the scenario in which the same amount of SOC increase in the depth of 0-25 cm was  
 514      simulated but without subsoil SOC depletion (Figure 5). We emphasize that, from the  
 515      point of view of water availability to plants with deep roots, management strategies should  
 516      aim at increasing SOC content deeper than only in the topsoil.

517      According to Bai et al. (2019), reduced tillage or no-till increases SOC mostly  
 518      in the top 10 cm and also in the sub-soil below 50 cm. The same study found that cover-  
 519      cropping could increase SOC down to 70 cm depth. Incorporation of perennial grasses  
 520      into crop rotations could help increase SOC to 60 cm depth, beyond the plough layer

521 (Carter and Gregorich, 2010). Evidence of this under Swiss conditions was provided by  
522 Guillaume et al. (2021); Guillaume et al. (2022). Overall, such strategies were found to  
523 be most beneficial to SOC accumulation near the soil surface (Bai et al., 2019). One  
524 management operation that could effectively contribute to an accumulation of SOC in  
525 deeper soil layers is deep ploughing (Alcántara et al., 2016). However, when the soil is  
526 loosened the SOC oxidation process is enhanced, as well as erosion may be triggered,  
527 which has to be accounted for when planning such interventions.

528 We have tested the scenario of incorporating extra amount of SOC in the soil  
529 down to a depth of 135 cm. This is a scenario that would require similar strategies as the  
530 previously discussed scenario, but it is likely rather difficult to implement, especially with  
531 greater amounts of SOC stored. Our study showed that in terms of water-availability to  
532 the (maize) crop, this scenario has little extra benefit to offer over the scenario of having  
533 extra SOC sequestered to 65 cm depth. Hence, any investment in sequestering SOC into  
534 such depths should not be driven by high expectation of hydrological benefits.

535

### 536 **6.3 Limitations and further work**

537 Our study, as well as previous modelling studies exploring impacts of SOC  
538 additions on soil water availability (e.g. Ankenbauer and Loheide (2017), Bonfante et al.  
539 (2020), Feng et al. (2022)), build on pedotransfer functions that are believed to be best in  
540 estimating soil hydraulic parameters for the study area based on levels of SOC and other  
541 soil properties. The selection of PTFs, however, may play a crucial role in the outcome  
542 of simulated scenarios. While recent studies confirm the validity of the equations used  
543 (e.g. Nasta et al. (2021); Wagner et al. (2004)), uncertainties in derived estimates may  
544 still be large (Fatichi et al., 2020). PTF structure may also have an influence in that more

545 advanced (aka. “better”) PTFs are usually products of refined machine learning  
546 algorithms that may produce strong results in general but may have different estimation  
547 qualities in different parts of the data domain. Since such local performance is rarely  
548 evaluated, future work should thus explore the sensitivity of SOC benefits via using an  
549 ensemble of PTFs. Moreover, measurements of soil hydraulic properties in combination  
550 with SOC, texture and bulk density in long term field trials investigating management  
551 alternatives affecting SOC would provide very useful evidence to help disentangle the  
552 effects of land use and management on the relationships between soil texture and  
553 hydraulic properties. By integrating management and also local climate information in  
554 PTFs, their uncertainties in predicting soil hydraulic properties in specific context could  
555 be reduced (Van Looy et al., 2017). Many historic records do not provide sufficient  
556 information on how certain measurements were performed, or when the samples were  
557 taken. Also, the timing of field sampling is likely to play a role here, as it is known that  
558 soil hydraulic properties vary in time and are influenced e.g. by precipitation regime or  
559 land use and management (Caplan et al., 2019; Lu et al., 2020).

560 In this study, we focused on transpiration reduction, which is likely to imply  
561 biomass reduction, but may not necessarily imply yield reduction – depending on the  
562 timing of water stress. Other studies have investigated impacts of CC on yields for grain  
563 maize in Switzerland (Holzkämper, 2020; Holzkämper et al., 2015a) and it was found that  
564 yield trends differ depending on the choice of varieties assumed to be planted. In our  
565 study here, we focus on drought impacts on crop transpiration alone. Subsequent yield  
566 formation will be affected by crop transpiration, but also by various other drivers (e.g.  
567 temperature & radiation limitations, timing of stresses, heat stress). In order to obtain a  
568 clearer view on the impacts of SOC increases on crop transpiration, we elected not to  
569 consider the multitude of such interactive effects in the presented study. In future work,

570 it will be interesting to explore possibilities to further increase the benefits of SOC  
571 additions by combining that strategy with other adaptations of crop and soil management  
572 (e.g. earlier maturing varieties, cover cropping, mulching of soil to reduce evaporation).  
573 In this context, it will be advisable to also account for a dynamic development of  
574 phenology and thus leaf area index to account for possible interactions between crop  
575 growth and soil moisture conditions.

576 While our study focused solely on the impacts of SOC additions on soil water  
577 dynamics, SOC increases could have additional benefits for crop productivity and yield  
578 stability by feeding and supporting beneficial microbial communities in the soil (e.g.  
579 rhizobacteria, nitrogen-fixing bacteria, and mycorrhizal fungi), which increase the crops'  
580 ability to take up water and nutrients (Coban et al., 2022; Renwick et al., 2021;  
581 Kallenbach and Grandy, 2011). Such aspects could be addressed in future field  
582 experimental studies. Beyond that, future field- and model-based studies may also  
583 evaluate trade-offs or synergies of SOC promoting management strategies with regard to  
584 other soil-related ecosystem service indicators such as nitrate leaching, soil loss or runoff  
585 generation to provide insights regarding the possibilities to increase the sustainability of  
586 agricultural production overall (Bonfante et al., 2019). Alternative modelling approaches  
587 considering dynamic changes in soil hydraulic properties could also be applied in the  
588 future to investigate the influence of soil structural dynamics on the adaptation benefits  
589 of SOC accumulation (e.g. based on Meurer et al. (2020b), Meurer et al. (2020a)), as to  
590 our understanding, current models do not facilitate the representation of soil as a  
591 temporally variable medium.

592

593 **7. Conclusions**

594 Our study is the first to investigate the possibilities to reduce  $T_{redry}$ , an indicator  
 595 of drought stress, in maize cultivated in the Swiss Central Plateau through increasing SOC  
 596 in the top- and subsoil. Our simulations showed that  $T_{redry}$  in maize is expected to  
 597 increase with climate change in the Swiss Central Plateau region, by around 60-65 mm  
 598 irrespective of SOC increase. Increasing SOC in a typical agricultural soil in Switzerland,  
 599 however, is beneficial to reduce drought limitations in maize, showed by consistently  
 600 positive average transpiration gains. These benefits are minimal if SOC is only increased  
 601 in the top 25 cm, but become considerable if SOC is increased down to 65- or 135 cm  
 602 depth. With a 2% addition of SOC down to 65cm depth, a considerable average  
 603 transpiration gain of 40 mm can be reached. This scenario can be achievable considering  
 604 management adaptations such as cover cropping or compost applications. It appears that  
 605 a greater or deeper SOC addition would not return substantial extra benefits in terms of  
 606 offsetting more crop drought stress rooting in the changing climate.

607

608 **8. Author contribution**

609 Conceptualization<sup>1,3</sup>, Data curation<sup>1</sup>, Formal analysis<sup>1,3</sup>, Funding acquisition<sup>3</sup>,  
 610 Investigation<sup>1,2,3</sup>, Methodology<sup>1,3</sup>, Resources<sup>3</sup>, Software<sup>1</sup>, Visualization<sup>1</sup>, Writing –  
 611 original draft preparation<sup>1,3</sup>, Writing – review & editing<sup>1,2,3</sup>.

612 <sup>1</sup>MET; <sup>2</sup>AN; <sup>3</sup>AH

613 **9. Competing interests**

614 The authors declare that they have no conflict of interest.

615 **10. Acknowledgments**

616 This project was developed in the framework of the OPTAIN and SoilX-EJP SOIL  
 617 projects. OPTAIN (OPTimal strategies to retAIN and re-use water and nutrients in small  
 618 agricultural catchments across different soil-climatic regions in Europe, [cordis.europa.eu](http://cordis.europa.eu))

619 has received funding from the European Union's Horizon 2020 research and innovation  
 620 programme (Grant Agreement N° 862756). SoilX is part of the European Joint Program  
 621 for SOIL "Towards climate-smart sustainable management of agricultural soils" (EJP  
 622 SOIL) funded by the European Union Horizon 2020 research and innovation programme  
 623 (Grant Agreement N° 862695). The authors thank Dr. Volker Prasuhn for providing full  
 624 assistance with the lysimeter data.

625 **11. References**

626 Agroscope: Sortenversuche - Resultate Mais (In German), 2023.

627 Alcántara, V., Don, A., Well, R., and Nieder, R.: Deep ploughing increases agricultural  
 628 soil organic matter stocks, *Global Change Biology*, 22, 2939-2956,  
 629 <https://doi.org/10.1111/gcb.13289>, 2016.

630 Angers, D. A. and Eriksen-Hamel, N. S.: Full-Inversion Tillage and Organic Carbon  
 631 Distribution in Soil Profiles: A Meta-Analysis, *Soil Science Society of America Journal*,  
 632 72, 1370-1374, <https://doi.org/10.2136/sssaj2007.0342>, 2008.

633 Ankenbauer, K. J. and Loheide, S. P.: The effects of soil organic matter on soil water  
 634 retention and plant water use in a meadow of the Sierra Nevada, CA, *Hydrological  
 635 Processes*, 31, 891-901, 10.1002/hyp.11070, 2017.

636 Arthur, E., Tuller, M., Moldrup, P., and de Jonge, L. W.: Effects of biochar and manure  
 637 amendments on water vapor sorption in a sandy loam soil, *Geoderma*, 243-244, 175-  
 638 182, <https://doi.org/10.1016/j.geoderma.2015.01.001>, 2015.

639 BAFU: Hitze und Trockenheit im Sommer 2015. Auswirkungen auf Mensch und  
 640 Umwelt, Bern, 2016.

641 BAFU: Hitze und Trockenheit im Sommer 2018, Bern, 91, 2019.

642 Bai, X., Huang, Y., Ren, W., Coyne, M., Jacinthe, P.-A., Tao, B., Hui, D., Yang, J., and  
 643 Matocha, C.: Responses of soil carbon sequestration to climate-smart agriculture  
 644 practices: A meta-analysis, *Global Change Biology*, 25, 2591-2606,  
 645 <https://doi.org/10.1111/gcb.14658>, 2019.

646 Blanchy, G., Bragato, G., Di Bene, C., Jarvis, N., Larsbo, M., Meurer, K., and Garré, S.:  
 647 Soil and crop management practices and the water regulation functions of soils: a  
 648 qualitative synthesis of meta-analyses relevant to European agriculture, *SOIL*, 9, 1-20,  
 649 10.5194/soil-9-1-2023, 2023.

650 Bonfante, A., Basile, A., and Bouma, J.: Exploring the effect of varying soil organic  
 651 matter contents on current and future moisture supply capacities of six Italian soils,  
 652 *Geoderma*, 361, 10.1016/j.geoderma.2019.114079, 2020.

653 Bonfante, A., Terribile, F., and Bouma, J.: Refining physical aspects of soil quality and  
 654 soil health when exploring the effects of soil degradation and climate change on  
 655 biomass production: an Italian case study, *SOIL*, 5, 1-14, 10.5194/soil-5-1-2019, 2019.

656 Caplan, J. S., Giménez, D., Hirmas, D. R., Brunsell, N. A., Blair, J. M., and Knapp, A.  
 657 K.: Decadal-scale shifts in soil hydraulic properties induced by altered precipitation,  
 658 *Sci. Adv.*, 5, 2019.

659 Carter, M. R. and Gregorich, E. G.: Carbon and nitrogen storage by deep-rooted tall  
 660 fescue (*Lolium arundinaceum*) in the surface and subsurface soil of a fine sandy loam in  
 661 eastern Canada, *Agriculture, Ecosystems & Environment*, 136, 125-132,  
 662 <https://doi.org/10.1016/j.agee.2009.12.005>, 2010.

663 Coban, O., De Deyn, G. B., and van der Ploeg, M.: Soil microbiota as game-changers in  
 664 restoration of degraded lands, *Science*, 375, abe0725, doi:10.1126/science.abe0725,  
 665 2022.

666 Crystal-Ornelas, R., Thapa, R., and Tully, K. L.: Soil organic carbon is affected by  
 667 organic amendments, conservation tillage, and cover cropping in organic farming  
 668 systems: A meta-analysis, *Agriculture, Ecosystems & Environment*, 312, 107356,  
 669 <https://doi.org/10.1016/j.agee.2021.107356>, 2021.

670 de Wit, A., Boogaard, H., Fumagalli, D., Janssen, S., Knapen, R., van Kraalingen, D.,  
 671 Supit, I., van der Wijngaart, R., and van Diepen, K.: 25 years of the WOFOST cropping  
 672 systems model, *Agricultural Systems*, 168, 154-167,  
 673 <https://doi.org/10.1016/j.agsy.2018.06.018>, 2019.

674 Edeh, I. G., Mašek, O., and Buss, W.: A meta-analysis on biochar's effects on soil water  
 675 properties – New insights and future research challenges, *Science of The Total  
 676 Environment*, 714, 136857, <https://doi.org/10.1016/j.scitotenv.2020.136857>, 2020.

677 Eden, M., Gerke, H. H., and Houot, S.: Organic waste recycling in agriculture and  
 678 related effects on soil water retention and plant available water: a review, *Agronomy for  
 679 Sustainable Development*, 37, 11, 10.1007/s13593-017-0419-9, 2017.

680 FAO: World reference base for soil resources 2014. International soil classification  
 681 system for naming soils and creating legends for soil maps, FAO, 2015.

682 Faticchi, S., Or, D., Walko, R., Vereecken, H., Young, M. H., Ghezzehei, T. A., Hengl,  
 683 T., Kollet, S., Agam, N., and Avissar, R.: Soil structure is an important omission in  
 684 Earth System Models, *Nature Communications*, 11, 522, 10.1038/s41467-020-14411-z,  
 685 2020.

686 Feddes, R. A., Kowalik, P.J., Zaradny, H.: *Simulation of Field Water Use and Crop  
 687 Yield*, Wageningen, The Netherlands, 1978.

688 Feng, P., Wang, B., Harrison, M. T., Wang, J., Liu, K., Huang, M., Liu, D. L., Yu, Q.,  
 689 and Hu, K.: Soil properties resulting in superior maize yields upon climate warming,  
 690 *Agronomy for Sustainable Development*, 42, 85, 10.1007/s13593-022-00818-z, 2022.

691 Guillaume, T., Bragazza, L., Levasseur, C., Libohova, Z., and Sinaj, S.: Long-term soil  
 692 organic carbon dynamics in temperate cropland-grassland systems, *Agriculture,  
 693 Ecosystems & Environment*, 305, 107184, <https://doi.org/10.1016/j.agee.2020.107184>,  
 694 2021.

695 Guillaume, T., Makowski, D., Libohova, Z., Bragazza, L., Sallaku, F., and Sinaj, S.:  
 696 Soil organic carbon saturation in cropland-grassland systems: Storage potential and soil  
 697 quality, *Geoderma*, 406, 115529, <https://doi.org/10.1016/j.geoderma.2021.115529>,  
 698 2022.

699 Holzkämper, A.: Varietal adaptations matter for agricultural water use – a simulation  
 700 study on grain maize in Western Switzerland, *Agricultural Water Management*, 237,  
 701 106202, <https://doi.org/10.1016/j.agwat.2020.106202>, 2020.

702 Holzkämper, A., Calanca, P., and Fuhrer, J.: Identifying climatic limitations to grain  
 703 maize yield potentials using a suitability evaluation approach, *Agricultural and Forest  
 704 Meteorology*, 168, 149-159, <https://doi.org/10.1016/j.agrformet.2012.09.004>, 2013.

705 Holzkämper, A., Calanca, P., Honti, M., and Fuhrer, J.: Projecting climate change  
 706 impacts on grain maize based on three different crop model approaches, *Agricultural  
 707 and Forest Meteorology*, 214-215, 219-230,  
 708 <https://doi.org/10.1016/j.agrformet.2015.08.263>, 2015a.

709 Holzkämper, A., Fossati, D., Hiltbrunner, J., and Fuhrer, J.: Spatial and temporal trends  
 710 in agro-climatic limitations to production potentials for grain maize and winter wheat in  
 711 Switzerland, *Regional Environmental Change*, 15, 109-122, 10.1007/s10113-014-0627-  
 72 7, 2015b.

713 IPCC: P.R. Shukla, J. Skea, R. Slade, R. van Diemen, E. Haughey, J. Malley, M.  
 714 Pathak, J. Portugal Pereira (Eds.). Technical Summary, in: *Climate Change and Land:  
 715 an IPCC special report on climate change, desertification, land degradation, sustainable*

716 land management, food security, and greenhouse gas fluxes in terrestrial ecosystems,  
 717 edited by: Shukla, P. R., Skea, J., Buendia, E. C., Masson-Delmotte, V., Pörtner, H.-O.,  
 718 Roberts, D. C., Zhai, P., Slade, R., Connors, S., Diemen, R. v., Ferrat, M., Haughey, E.,  
 719 Luz, S., Neogi, S., Pathak, M., Petzold, J., Pereira, J. P., Vyas, P., Huntley, E., Kissick,  
 720 K., Belkacemi, M., and Malley, J., In press, 2019.

721 Jarvis, N., Koestel, J., Messing, I., Moeys, J., and Lindahl, A.: Influence of soil, land  
 722 use and climatic factors on the hydraulic conductivity of soil, *Hydrol. Earth Syst. Sci.*,  
 723 17, 5185-5195, 10.5194/hess-17-5185-2013, 2013.

724 Kallenbach, C. and Grandy, A. S.: Controls over soil microbial biomass responses to  
 725 carbon amendments in agricultural systems: A meta-analysis, *Agriculture, Ecosystems  
 726 & Environment*, 144, 241-252, <https://doi.org/10.1016/j.agee.2011.08.020>, 2011.

727 Kan, Z.-R., Ma, S.-T., Liu, Q.-Y., Liu, B.-Y., Virk, A. L., Qi, J.-Y., Zhao, X., Lal, R.,  
 728 and Zhang, H.-L.: Carbon sequestration and mineralization in soil aggregates under  
 729 long-term conservation tillage in the North China Plain, *CATENA*, 188, 104428,  
 730 <https://doi.org/10.1016/j.catena.2019.104428>, 2020.

731 Kotlarski, S. and Rajczak, J.: CH2018 - Climate Scenarios for Switzerland.  
 732 Documentation of the localized CH2018 datasets., National Centre for Climate Services  
 733 - Switzerland, 2018.

734 Krauss, M., Wiesmeier, M., Don, A., Cuperus, F., Gattinger, A., Gruber, S., Haagsma,  
 735 W. K., Peigné, J., Palazzoli, M. C., Schulz, F., van der Heijden, M. G. A., Vincent-  
 736 Caboud, L., Wittwer, R. A., Zikeli, S., and Steffens, M.: Reduced tillage in organic  
 737 farming affects soil organic carbon stocks in temperate Europe, *Soil and Tillage  
 738 Research*, 216, 105262, <https://doi.org/10.1016/j.still.2021.105262>, 2022.

739 Kroes, J. G., Dam, J. C. v., Bartholomeus, R. P., Groenendijk, P., Heinen, M., Hendriks,  
 740 R. F. A., Mulder, H. M., Supit, I., and Walsum, P. E. V. v.: SWAP version 4 Theory  
 741 description and user manual, Report 2780, 2017.

742 Lal, R.: World cropland soils as a source or sink for atmospheric carbon, in: *Advances  
 743 in Agronomy*, Academic Press, 145-191, [https://doi.org/10.1016/S0065-2113\(01\)71014-0](https://doi.org/10.1016/S0065-2113(01)71014-0), 2001.

745 Lal, R.: Soil carbon sequestration to mitigate climate change, *Geoderma*, 123, 1-22,  
 746 <https://doi.org/10.1016/j.geoderma.2004.01.032>, 2004.

747 Larsbo, M., Koestel, J., Kätterer, T., and Jarvis, N.: Preferential Transport in  
 748 Macropores is Reduced by Soil Organic Carbon, *Vadose Zone Journal*, 15,  
 749 vzb2016.2003.0021, <https://doi.org/10.2136/vzb2016.03.0021>, 2016.

750 Libohova, Z., Seybold, C., Wysocki, D., Wills, S., Schoeneberger, P., Williams, C.,  
 751 Lindbo, D., Stott, D., and Owens, P. R.: Reevaluating the effects of soil organic matter  
 752 and other properties on available water-holding capacity using the National Cooperative  
 753 Soil Survey Characterization Database, *Journal of Soil and Water Conservation*, 73,  
 754 411-421, 10.2489/jswc.73.4.411, 2018.

755 Liu, S., Lei, Y., Zhao, J., Yu, S., and Wang, L.: Research on ecosystem services of  
 756 water conservation and soil retention: a bibliometric analysis, *Environmental Science  
 757 and Pollution Research*, 28, 2995-3007, 10.1007/s11356-020-10712-4, 2021.

758 Lu, J., Zhang, Q., Werner, A. D., Li, Y., Jiang, S., and Tan, Z.: Root-induced changes of  
 759 soil hydraulic properties – A review, *Journal of Hydrology*, 589, 125203,  
 760 <https://doi.org/10.1016/j.jhydrol.2020.125203>, 2020.

761 Maharjan, G. R., Prescher, A.-K., Nendel, C., Ewert, F., Mboh, C. M., Gaiser, T., and  
 762 Seidel, S. J.: Approaches to model the impact of tillage implements on soil physical and  
 763 nutrient properties in different agro-ecosystem models, *Soil and Tillage Research*, 180,  
 764 210-221, <https://doi.org/10.1016/j.still.2018.03.009>, 2018.

765 Meurer, K. H. E., Chenu, C., Coucheney, E., Herrmann, A. M., Keller, T., Kätterer, T.,  
 766 Nimblad Svensson, D., and Jarvis, N.: Modelling dynamic interactions between soil  
 767 structure and the storage and turnover of soil organic matter, *Biogeosciences*, 17, 5025-  
 768 5042, 10.5194/bg-17-5025-2020, 2020a.

769 Meurer, K. H. E., Barron, J., Chenu, C., Coucheney, E., Fielding, M., Hallett, P.,  
 770 Herrmann, A. M., Keller, T., Koestel, J., Larsbo, M., Lewan, E., Or, D., Parsons, D.,  
 771 Parvin, N., Taylor, A., Vereecken, H., and Jarvis, N.: A framework for modelling soil  
 772 structure dynamics induced by biological activity, *Global Change Biology*, 26, 5382-  
 773 5403, <https://doi.org/10.1111/gcb.15289>, 2020b.

774 Minasny, B. and McBratney, A. B.: Limited effect of organic matter on soil available  
 775 water capacity, *European Journal of Soil Science*, 69, 39-47, 10.1111/ejss.12475, 2017.

776 Minasny, B., Malone, B. P., McBratney, A. B., Angers, D. A., Arrouays, D., Chambers,  
 777 A., Chaplot, V., Chen, Z.-S., Cheng, K., Das, B. S., Field, D. J., Gimona, A., Hedley, C.  
 778 B., Hong, S. Y., Mandal, B., Marchant, B. P., Martin, M., McConkey, B. G., Mulder, V.  
 779 L., O'Rourke, S., Richer-de-Forges, A. C., Odeh, I., Padarian, J., Paustian, K., Pan, G.,  
 780 Poggio, L., Savin, I., Stolbovoy, V., Stockmann, U., Sulaeman, Y., Tsui, C.-C., Vågen,  
 781 T.-G., van Wesemael, B., and Winowiecki, L.: Soil carbon 4 per mille, *Geoderma*, 292,  
 782 59-86, <https://doi.org/10.1016/j.geoderma.2017.01.002>, 2017.

783 Modak, K., Ghosh, A., Bhattacharyya, R., Biswas, D. R., Das, T. K., Das, S., and Singh,  
 784 G.: Response of oxidative stability of aggregate-associated soil organic carbon and deep  
 785 soil carbon sequestration to zero-tillage in subtropical India, *Soil and Tillage Research*,  
 786 195, 104370, <https://doi.org/10.1016/j.still.2019.104370>, 2019.

787 Mualem, Y.: A new model for predicting the hydraulic conductivity of unsaturated  
 788 porous media, *Water Resources Research*, 12, 513-522,  
 789 <https://doi.org/10.1029/WR012i003p00513>, 1976.

790 Murphy, B.: Key soil functional properties affected by soil organic matter - evidence  
 791 from published literature, *IOP Conference Series: Earth and Environmental Science*, 25,  
 792 012008, 10.1088/1755-1315/25/1/012008, 2015.

793 Nasta, P., Szabó, B., and Romano, N.: Evaluation of pedotransfer functions for  
 794 predicting soil hydraulic properties: A voyage from regional to field scales across  
 795 Europe, *Journal of Hydrology: Regional Studies*, 37, 10.1016/j.ejrh.2021.100903, 2021.

796 Nemes, A., Rawls, W. J., and Pachepsky, Y. A.: Influence of Organic Matter on the  
 797 Estimation of Saturated Hydraulic Conductivity, *Soil Science Society of America  
 798 Journal*, 69, 1330-1337, <https://doi.org/10.2136/sssaj2004.0055>, 2005.

799 Prasuhn, V., Humphys, C., and Spiess, E.: Seventy-Two Lysimeters for Measuring  
 800 Water Flows and Nitrate Leaching under Arable Land, *NAS International Workshop on  
 801 Applying the Lysimeter Systems to Water and Nutrient Dynamics*, Wanju, Korea,  
 802 Rawls, W. J., Nemes, A., and Pachepsky, Y.: Effect of soil organic carbon on soil  
 803 hydraulic properties, in: *Developments in Soil Science*, Elsevier, 95-114,  
 804 [https://doi.org/10.1016/S0166-2481\(04\)30006-1](https://doi.org/10.1016/S0166-2481(04)30006-1), 2004.

805 Renwick, L. L. R., Deen, W., Silva, L., Gilbert, M. E., Maxwell, T., Bowles, T. M., and  
 806 Gaudin, A. C. M.: Long-term crop rotation diversification enhances maize drought  
 807 resistance through soil organic matter, *Environmental Research Letters*, 16, 084067,  
 808 10.1088/1748-9326/ac1468, 2021.

809 Rivier, P.-A., Jamniczky, D., Nemes, A., Makó, A., Barna, G., Uzinger, N., Rékási, M.,  
 810 and Farkas, C.: Short-term effects of compost amendments to soil on soil structure,  
 811 hydraulic properties, and water regime, *Journal of Hydrology and Hydromechanics*, 70,  
 812 74-88, doi:10.2478/johh-2022-0004, 2022.

813 Smith, P., Martino, D., Cai, Z., Gwary, D., Janzen, H., Kumar, P., McCarl, B., Ogle, S.,  
 814 O'Mara, F., Rice, C., Scholes, B., Sirotenko, O., Howden, M., McAllister, T., Pan, G.,

815 Romanenkov, V., Schneider, U., Towprayoon, S., Wattenbach, M., and Smith, J.:  
816 Greenhouse gas mitigation in agriculture, Philosophical Transactions of the Royal  
817 Society B: Biological Sciences, 363, 789-813, doi:10.1098/rstb.2007.2184, 2008.  
818 Szabó, B., Weynans, M., and Weber, T. K. D.: Updated European hydraulic  
819 pedotransfer functions with communicated uncertainties in the predicted variables  
820 (euptfv2), Geoscientific Model Development, 14, 151-175, 10.5194/gmd-14-151-2021,  
821 2021.  
822 Topa, D., Cara, I. G., and Jităreanu, G.: Long term impact of different tillage systems on  
823 carbon pools and stocks, soil bulk density, aggregation and nutrients: A field meta-  
824 analysis, CATENA, 199, 105102, <https://doi.org/10.1016/j.catena.2020.105102>, 2021.  
825 van Genuchten, M. T.: A Closed-form Equation for Predicting the Hydraulic  
826 Conductivity of Unsaturated Soils, Soil Science Society of America Journal, 44, 892-  
827 898, 10.2136/sssaj1980.03615995004400050002x, 1980.  
828 Van Looy, K., Bouma, J., Herbst, M., Koestel, J., Minasny, B., Mishra, U., Montzka,  
829 C., Nemes, A., Pachepsky, Y. A., Padarian, J., Schaap, M. G., Tóth, B., Verhoef, A.,  
830 Vanderborght, J., van der Ploeg, M. J., Weihermüller, L., Zacharias, S., Zhang, Y., and  
831 Vereecken, H.: Pedotransfer Functions in Earth System Science: Challenges and  
832 Perspectives, Reviews of Geophysics, 55, 1199-1256,  
833 <https://doi.org/10.1002/2017RG000581>, 2017.  
834 Wagner, B., Tarnawski, V. R., and Stöckl, M.: Evaluation of pedotransfer functions  
835 predicting hydraulic properties of soils and deeper sediments, Journal of Plant Nutrition  
836 and Soil Science, 167, 236-245, <https://doi.org/10.1002/jpln.200321251>, 2004.  
837 Wang, T., Wedin, D., and Zlotnik, V. A.: Field evidence of a negative correlation  
838 between saturated hydraulic conductivity and soil carbon in a sandy soil, Water  
839 Resources Research, 45, <https://doi.org/10.1029/2008WR006865>, 2009.  
840 Weber, T. K. D., Weynans, M., and Szabó, B.: R package of updated European  
841 hydraulic pedotransfer functions (euptf2), 10.5281/zenodo.4281045, 2020.  
842 Zhang, X., Jia, J., Chen, L., Chu, H., He, J.-S., Zhang, Y., and Feng, X.: Aridity and  
843 NPP constrain contribution of microbial necromass to soil organic carbon in the  
844 Qinghai-Tibet alpine grasslands, Soil Biology and Biochemistry, 156, 108213,  
845 <https://doi.org/10.1016/j.soilbio.2021.108213>, 2021.  
846  
847